

The frequency of nuclear star-formation in Seyfert 2 galaxies

Thaïsa Storchi-Bergmann^{1,2}, Daniel Raimann^{2,3}, Eduardo L. D. Bica² and Henrique A. Fraquelli^{2,3}

Instituto de Física – UFRGS, CP 15051, CEP 91501-970, Porto Alegre, RS, Brasil

thaisa@if.ufrgs.br

Received _____; accepted _____

Submitted to The Astrophysical Journal

¹Visiting Astronomer at the Cerro Tololo Interamerican Observatory, operated by the Association of Universities for Research in Astronomy, Inc. under contract with the National Science Foundation.

²e-mail addresses: thaisa@if.ufrgs.br, raimann@if.ufrgs.br, bica@if.ufrgs.br, ico@if.ufrgs.br

³CNPq Fellow

ABSTRACT

We investigate the detectability of starburst signatures in the nuclear spectrum of Seyfert 2 galaxies by constructing spectral models in the wavelength range $\lambda\lambda 3500\text{--}4100\text{\AA}$, combining the spectrum of a bulge population (of age ≈ 10 Gyr) with that of younger stellar populations, spanning ages from ≈ 3 Myr to 1 Gyr. The major constraints in the analysis are: (i) the continuum ratio $3660\text{\AA}/4020\text{\AA}$, which efficiently discriminates between models combining a bulge spectrum with a stellar population younger than ≈ 50 Myr and those with older stellar populations; (ii) the presence of the Balmer lines H8, H9 and H10 in absorption, which are unambiguous signatures of stellar populations with ages in the range 10 Myr–1 Gyr for the relevant metallicities. Their detectability depends both on the age of the young component and on its contribution to the total flux relative to that of the bulge.

We also construct models combining the bulge template with a power-law (PL) continuum, which is observed in some Seyfert 2's in polarized light, contributing with typically 10–40% of the flux at $\lambda 4020\text{\AA}$. We conclude that such continuum cannot be distinguished from that of a very young stellar population (age ≤ 10 Myr), contributing with less than $\approx 0.02\%$ of the mass of the bulge.

The models are compared with nuclear spectra — corresponding to a radius of 200–300 pc at the galaxy — of 20 Seyfert 2 galaxies, in which we specifically look for the signatures above of young to intermediate age stellar populations. We find them in ten galaxies, thus 50% of the sample. But only in six cases (30% of the sample) they can be attributed to young stars (age < 500 Myr): Mrk 1210, ESO 362-G8, NGC 5135, NGC 5643, NGC 7130 and NGC 7582. In the remaining four cases, the signatures are due to intermediate age stars (≈ 1 Gyr).

We find a tendency for the young stars to be found more frequently among

the late type Seyfert’s. This tendency is supported by a comparison between the equivalent widths (W) of absorption lines of the nuclear spectra of the Seyfert 2’s with those of normal galaxies of the same Hubble type: for the late-type (Sb or later), the W values of the Seyfert’s are within the observed range of the normal galaxies, while the W values are lower than those of the normal galaxies for 7 out of the 11 early-type galaxies (S0 and Sa).

1. Introduction

The connection between star-formation and nuclear activity in galaxies has been the subject of a number of recent studies. On the theoretical side, models such as those of Perry & Dyson (1985) and Norman & Scoville (1988) propose that a nuclear young stellar cluster is the reservoir of fuel for the AGN in the nucleus.

On the observational side, Terlevich, Diaz & Terlevich (1990) have argued that for a number of Seyfert 2 galaxies, circumnuclear starbursts are necessary to explain the strength of the CaII triplet (at $\lambda \approx 8500\text{\AA}$) in absorption. Starbursts have also been proposed as the source of the blue unpolarized continuum observed in Seyfert 2 galaxies (FC2, Tran 1995a,b,c) by Cid Fernandes & Terlevich (1992, 1995). Heckman et al. (1995) have proposed the same on the basis of the IUE spectra of the brightest Seyfert 2 galaxies in the UV. Detailed studies of individual cases have been performed by Heckman et al. (1997) who have shown HST UV images and spectra of the circumnuclear starburst around Mrk 477, and González Delgado et al. (1998), who has analyzed similar data for the starbursts around the Seyfert 2 nuclei of NGC 7130, NGC 5135 and IC 3639. The latter studies have shown the most unambiguous signatures of massive starbursts around these nuclei, but have been performed for only 4 galaxies.

Our main goal in this work is to extend to a larger sample the search of such nuclear starbursts signatures in AGN's. Recent works (e.g. González Delgado, Leitherer & Heckman 1999) have pointed out that some of the best spectral features to date starbursts are found in the blue-near UV spectral region (3400–4200Å), the strongest being the higher order Balmer absorption lines (hereafter HOBL). These features seem indeed to be present in the spectra of most starburst galaxies, as can be observed in the sample of Storchi-Bergmann, Kinney & Challis (1995). Bica, Alloin & Schmitt (1994, hereafter BAS94) have also pointed out the importance of this spectral range for the interpretation of composite stellar populations because of the signatures of the younger components (e.g. Balmer lines and Balmer jump), and the 4000Å break related to the old and intermediate age ($\approx 1\text{--}5$ Gyr) populations. They studied near-UV/blue spectra of star clusters of all ages, and analyzed equivalent widths of a number of features and continuum fluxes as a function of age and metallicity. Fig. 1 of BAS94 is particularly illustrative of the variation of the HOBL as a function of age and metallicity.

In order to look for starbursts in Seyfert's, one has to take into account the contribution of the underlying bulge population. Simulations of starburst spectra superimposed on older stellar populations, for the spectral range 3700–9600Å were carried out by Bica, Alloin & Schmidt (1990, hereafter BAS90; see also Schmidt, Alloin & Bica 1995). For 3 relative amounts of mass stocked in star formation events, they combined a bulge spectrum with spectra of star cluster templates of different ages to simulate the evolution of equivalent widths and continuum fluxes. In the present study, we construct similar models in the range 3600–4100Å which is particularly important for the Seyfert 2 issue. The present models represent an improvement relative to BAS90 in the sense that the templates incorporate the high S/N near-UV range constructed from the star cluster spectra of BAS94.

We then apply the results of the above simulations to the nuclear spectra of 20

Seyfert 2 galaxies in order to quantify the contribution of a possible nuclear starburst to the spectrum. The data used here are the nuclear spectra of the 20 Seyfert 2's of the sample of Cid Fernandes, Schmitt & Storchi-Bergmann (1998). Schmitt, Storchi-Bergmann & Cid Fernandes (1999) have performed a spectral synthesis using these spectra, but most features used in the synthesis have $\lambda > 4000\text{\AA}$. Our goal here is to take a close look at the near-UV region. The aperture used in the extraction of the nuclear spectra ($2'' \times 2''$) corresponds at the galaxy to regions within a radius 200–300 pc from the nucleus, which are of the order of the nuclear starburst sizes investigated in detail by González Delgado et al. (1998).

The second goal of the present study is to compare the results obtained for the Seyferts with those for normal galaxies of the same Hubble type. Cid Fernandes et al. (1998) have shown that in many Seyfert 2's the blue nuclear continuum seems to be absent, when one takes into account the surrounding stellar population. In other words, they have found that the nuclear stellar population is varied, and usually differs from that of an elliptical galaxy, as adopted in early works. The blue continuum artificially appears when one subtracts an elliptical galaxy template from the nuclear spectrum of a galaxy containing some contribution of younger stars (Storchi-Bergmann, Cid Fernandes & Schmitt 1998). The spectral syntheses of Schmitt et al. (1999) have further shown that the main difference between the nuclear stellar population of Seyfert 2's and that of an elliptical galaxy is an excess contribution of a ≈ 100 Myr stellar population. These findings point to FC2 as due to young stars in several cases, but another important question is whether the contribution of young stars in Seyfert nuclei is larger than that in normal galaxies of the same Hubble type. Since Seyfert nuclei as a rule occur in spiral galaxies, some contribution of young stars is expected. In order to access this aspect, it is necessary to compare the nuclear stellar population characteristics of the Seyfert's with those of normal galaxies. We thus assume the spectral study of Bica & Alloin (1987) as representative of the results obtained for normal galaxies to make such a comparison.

The paper is organized as follows: in Section 2 we discuss the near-UV features and adopted templates; in Sec. 3 we present the spectral models; in Sec. 4 we compare the nuclear Seyfert 2 spectra with the models; in Sec. 5 we compare our results with those of similar studies; in Sec. 6 we discuss the degeneracy problem between a featureless power-law and a very young starburst continuum; in Sec. 7 we compare the results for the Seyfert’s with those for normal galaxies of the same Hubble type, and finally in Sec. 8 we present our conclusions.

2. Near-UV features and adopted templates

The spectral features in the near-UV for a red (old/intermediate age) stellar population are markedly different from those of younger stellar populations. This can be observed in Fig. 1 (see also Fig. 2 of BAS94), where we show the stellar population templates used in this blue-violet study. The star cluster and early-type galaxy bulge (E2E5 of BAS94) templates used here incorporate observations from near-UV and visible (Bica & Alloin 1986, 1987) domains. The templates also extend further to the UV and near-IR domains, which can be used as additional constraints in the analysis. A detailed description of these templates is given by Bica and collaborators in Section 4.1 of Leitherer et al. (1996). To represent a 3 Myr stellar population we adopt the integrated spectrum of 30 Doradus (BAS94, Bica & Alloin 1986).

In the old stellar population template, typical of elliptical galaxies or of the bulge of spirals, the main absorption features are the CaII K ($\lambda 3933\text{\AA}$) and H ($\lambda 3970\text{\AA}$) lines and a blend of absorptions due to CN, MgI, SiI and FeI. For the younger stellar populations, with ages between 10 Myr and 1 Gyr, the main features are, apart from the CaII K and H lines with varying strengths, the high order Balmer lines in absorption, in particular H δ ($\lambda 4102\text{\AA}$), H ϵ ($\lambda 3970\text{\AA}$), H8 ($\lambda 3889\text{\AA}$), H9 ($\lambda 3835\text{\AA}$) and H10 ($\lambda 3797\text{\AA}$). Detection of the

latter lines in a spectrum is thus a strong signature of the presence of a blue (young) stellar population, except when the burst is younger than 5 Myrs, in which case these absorptions are filled by emission.

3. Models

Following BAS90, we have used the template bulge spectra in combination with varying proportions of the younger templates in order to build simple model spectra representative of composite populations. We have combined the bulge component with 0.1%, 1% and 10% mass contributions locked in the younger components, to construct the models shown in Figs. 2, 3 and 4. The adopted mass-to-light ratios in V (BAS90) for the templates representing bursts of different ages, together with the relative luminosities at $\lambda 4020\text{\AA}$ $L_{\lambda 4020}$ for bursts of equal masses, are listed in Table 1. This table can be used to find the contribution in flux at $\lambda 4020\text{\AA}$ corresponding to a given mass proportion. For example, in order to construct the model combining the bulge with 0.1% in mass of the 10 Myr population, we have multiplied $L_{\lambda 4020}$ of the 10 Myr template by 0.1% to obtain 3.354, which is the normalization factor of the template at $\lambda 4020\text{\AA}$. Subsequently it is added to the bulge template normalized to 1 at this same wavelength. Notice that for equal masses, the 10 Myr cluster $L_{\lambda 4020}$ value is higher than that of the 3 Myr cluster embedded in the HII region because of the appearance of supergiants.

By examining the characteristic features of the young stars in Figs. 2, 3, and 4, in particular the absorption lines H8, H9 and H10 (the HOBL) – which are the ones less affected by emission in Seyfert’s, see below – it can be concluded that: (i) if the starburst is very young, with ages of a few Myrs, the HOBL are filled by emission; in this case, the HII region emission spectrum may be used as constraint; (ii) for a small starburst, so that its mass is $\approx 0.1\%$ of that of the bulge, the HOBL can be detected for young starbursts with

ages from 10 to 50 Myrs; (iii) for a starburst corresponding to 1% of the mass of the old stars, the above features can be observed for ages from 10 to 500 Myrs; (iv) for a stronger starburst, corresponding to 10% of the mass of the bulge, the features are observed for ages from 10 Myrs up to 1 Gyr.

In order to quantitatively characterize stellar populations, BAS94 have proposed the use of a few continuum points, whereby a continuum is traced (connecting these points using straight lines) to measure the equivalent widths (hereafter represented by W) of a number of features. However, in Seyferts, many of these features are filled by emission lines and cannot be used. By comparing the above stellar population templates with typical Seyfert spectra, we conclude that the windows which are usually free from emission-lines are $\lambda\lambda 3810\text{--}3822\text{\AA}$ (centered on a continuum point), $\lambda\lambda 3822\text{--}3858\text{\AA}$ (centered on H9) and $\lambda\lambda 3908\text{--}3952\text{\AA}$ (centered on the CaII K line). We have thus followed the BAS90's method to construct the continuum, and measured the W 's within the three windows above, hereafter identified as W_C , W_{H9} and W_{CaK} , respectively. Fig. 5 illustrates the continuum and windows used for three Seyfert 2's with distinct near-UV spectra.

The near-UV W 's and continuum ratio $\lambda 3660/\lambda 4020$ (hereafter CR) were measured for the models. We show in Fig. 6 CR, W_C and W_{CaII} as a function of the young component's age, for the three proportions in mass above. It can be concluded that CR (F_{3660}/F_{4020}) is a powerful star-formation tracer for very young stellar populations, varying from 1.4 for a 3 Myr stellar population down to 0.6 for 50 Myrs or older. W_C and W_{CaIIK} are better age indicators for older bursts, but can trace stellar populations of all ages, from 3 Myr to 1 Gyr. We recall that blue-violet metal lines in composite spectra are age indicators because of the dilution effects caused by hot main sequence stars (Bica & Alloin 1986). Regarding H9, we conclude that its profile, together with those of the other HOBL are better age indicators than W_{H9} .

A number of Seyfert 2 galaxies present a polarized blue continuum with a power-law spectrum (Tran 1995a,b,c; Storchi-Bergmann et al. 1998). We have thus also constructed a second set of models combining the bulge template and a power-law $F_\nu \propto \nu^{-1.5}$ (hereafter PL), which is typical of the polarized continuum found by Tran (1995a,b,c). As the mass proportions used above have no meaning for the PL, we have used combinations with varying proportions of the PL in flux at $\lambda 4020\text{\AA}$.

The CR, W_C and W_{CaIIK} measured for the models combining the bulge template with the PL are plotted in Fig. 7, as a function of the PL percent contribution in flux at $\lambda 4020\text{\AA}$. As a comparison, we also plot the W values from models combining a bulge with the same flux contribution from a 10 Myr stellar population and a 100 Myr population. Combination with older populations produce similar CR values as the latter, as can be seen in Fig. 6. Fig. 7 shows that CR is the most powerful discriminator between a PL and bursts of ≈ 100 Myr or older. On the other hand, it shows also that a PL is hardly distinguishable from a 10 Myr burst on the basis of the CR and W values, a problem which has been already pointed out by several authors and by ourselves in Schmitt et al. (1999). We discuss this problem further in Sec. 6.

4. Comparison with Seyferts

The Seyfert sample used in this work is the same as that of Schmitt et al. (1999, hereafter SSC99) except for one radio-galaxy (with had a low signal-to-noise ratio spectrum in the near-UV), and consists of the 20 Seyfert 2's and 3 radio-galaxies from the larger sample of Cid Fernandes et al. (1998). As in SSC99, we use here only the nuclear spectra, extracted using windows of $2 \times 2''$, which correspond at the galaxy to regions of typical diameters of a few hundred parsecs.

These spectra are plotted in Figs. 8 to 12, separated according to the Hubble types. Here we have made use of the updated morphological classifications of our sample of Seyfert 2's in the Malkan et al. (1998) HST optical imaging survey, due to the better spatial resolution and dynamical range of their images as compared with those upon which the previous classifications (RC3, de Vaucouleurs et al. 1991) are based. We found an interesting result: out of the 20 galaxies in our sample, 10 have new classifications when compared with those of RC3, *always to later Hubble types*, as shown in Table 3. In particular, two of the galaxies with the most obvious signatures of recent star formation, NGC 5135 and NGC 7130 (González Delgado et al. 1998), previously classified as Sab and Sa, respectively, have been re-classified as Sc and Sd by Malkan et al. (1998).

The galaxies CR, W's and scales (pc/arcsec) are listed in Table 2. Typical errors are ~ 0.01 in CR and $\leq 1\text{\AA}$ in the W's. In Cid Fernandes et al. (1998) we have noticed that the nuclear spectra of these galaxies were in most cases redder than the extranuclear neighboring spectra, a result that we have attributed to reddening. Indeed, in the spectral syntheses performed by SSC99, they usually found significant reddenings ($0.1 \leq E(B-V) \leq 0.60$). We have thus corrected the nuclear spectra by the reddening (Seaton 1979) found by SSC99 before tracing the continuum and measuring the near-UV W's and CR. Notice however that the reddening corrections are not critical for CR due to the proximity of the continuum wavelengths $\lambda 3660\text{\AA}$ and $\lambda 4020\text{\AA}$.

We now compare the near-UV nuclear spectra of our sample with the synthetic spectra derived from the CR and W's listed in Table 2, using the model values from Figs. 6 and 7.

As the templates have lower spectral resolution ($\approx 15\text{\AA}$) than the Seyfert spectra ($\approx 5\text{\AA}$), we present here the models compared with the Seyfert spectra smoothed to better match the template resolution. The smoothing may cause loss of information, particularly when there are faint emission lines superimposed on the HOBL. We have thus always

checked for these emission lines at full resolution and have not included in the fit the absorption features affected by line emission. The most frequent case is the contamination of the $\text{CaII H} + \text{H}\epsilon$ absorption by $\text{NeIII}\lambda 3968 + \text{H}\epsilon$ emission.

Our goal with these comparisons is not a perfect match of the nuclear spectrum, but to identify the unambiguous signatures of the different components to the nuclear spectrum, looking in particular for the characteristic star-formation features HOBL (H8, H9 and H10 in absorption), using the simple models as a guide. With this approach, we also check if these simple models are a good representation of the nuclear stellar population. In applying the models of Figs. 6 and 7, it can be noted that the CR's and W's are compatible in several cases with more than one model. In these cases, the adopted model is the one which gives the best fit to the overall spectrum. The quality of the fit is inspected in regions free from emission lines, and the best fit is the one which gives the smaller residuals between the observed and model spectra in these regions.

As pointed out above, it is not possible to distinguish a PL continuum from that of a template of age 10 Myr or younger, for flux contributions smaller than 40% at $\lambda 4020\text{\AA}$. When such a continuum is needed we will call it PL/YS, meaning power-law or young stars. The nature of this component is further discussed in Sec. 6.

If the Seyfert 2 has strong Balmer emission-lines, the Balmer continuum in emission may be important in the near-UV region, diluting the W values calculated above. From the emission-line fluxes, we found that the Balmer continuum only contributes significantly (with more than 5% to the flux) for $\lambda < 3646\text{\AA}$, for the galaxies IC 1816, MCG 05-27-013, Mrk 348, Mrk 573 and Mrk 1210. In these cases we have considered also the contribution of the Balmer continuum, calculated as in Osterbrock (1989), and normalized according to the fluxes of the Balmer emission lines.

4.1. Elliptical galaxies

In order to verify the applicability of the templates as a basis to synthesize the Seyfert spectra, which were observed with the CTIO 4m Blanco telescope (Cid Fernandes et al. 1998), we have first applied the models to the normal elliptical galaxy IC 4889, observed with the same telescope, as a test to the method. In addition, we apply the models to three radio elliptical galaxies. The spectra and models are illustrated in Fig. 13.

4.1.1. *The normal elliptical IC 4889*

The near-UV W's and CR agree very well with those of the bulge template, and indicate no need of bluer components, as expected. Fig. 13a illustrates the observed spectrum as compared with the bulge template, showing a very good match of the observed spectrum to the template, indicating that we can use the templates constructed from the cluster spectra to synthesize the Seyfert nuclear spectra. Small differences are apparent in the CaIIK and H lines, which are deeper in the galaxy spectrum, even though the W's are the same as in the bulge template. We attribute this effect to a residual difference in spectral resolution between our spectrum and the bulge template.

4.1.2. *3C 33*

This is a radio galaxy with near-UV W values smaller than those of the bulge template, indicating the presence of some contribution of a blue component. The best fit for the spectrum is obtained with the combination of a bulge plus 10% in mass of a population of 1 Gyr, although the nuclear spectrum of the galaxy is still somewhat bluer for $\lambda < 3660 \text{ \AA}$. An improved fit to the blue end of the spectrum is obtained by adding a 5% contribution in flux at $\lambda 4020$ of the PL/YS component. The HOBL are at the detection limit (Fig. 13b).

NeIII λ 3968 + H ϵ emission can be observed filling the CaII H + H ϵ absorption.

4.1.3. *PKS 0349-27*

This radio galaxy has a small dilution of the W's when compared with the elliptical template values. The overall spectral distribution is best reproduced by the combination of the bulge with 10% flux contribution of the PL/YS component at λ 4020Å (Fig. 13c). The difference in the depth of the CaII K line is similar to that observed in IC 4889 and thus due to the better spectral resolution of the radio galaxy spectrum relative to the template. It is not possible to identify the HOBL. NeIII λ 3968 + H ϵ emission is filling the CaII H + H ϵ absorption.

4.1.4. *PKS 0634-20*

Here the case is similar to the one above, with a somewhat larger dilution in the continuum window and somewhat larger CR. The CR value indicates a 15% PL/YS contribution, in agreement with the W values and overall spectral distribution (Fig. 13d). The same remark above about the CaII K line applies here. It is not possible to identify the HOBL. There is contamination of the CaII H + H ϵ absorption by NeIII λ 3968 + H ϵ emission.

In summary, the near-UV spectrum of the three radio galaxies, when compared with normal ellipticals, shows a systematic need of a small (10-20% in flux at λ 4020Å) contribution of a blue component. For the 2 PKS sources, this component is well reproduced by a PL/YS continuum. For 3C 33 it is necessary to add also the contribution of a 1 Gyr stellar population with \approx 10% of the bulge component mass. A possible interpretation for such large intermediate age contribution would be the cannibalism of a small spiral galaxy

or magellan irregular, as is the case, for example, of the nearby radio galaxy Centaurus A (e.g. Storchi-Bergmann et al. 1997).

4.2. S0 and S0a

4.2.1. NGC 1358

In this galaxy the near-UV nuclear features and spectral distribution are well represented by the bulge template alone (Fig. 14a). There is some contamination of the CaII H + H ϵ absorption by NeIII λ 3968 + H ϵ emission.

4.2.2. NGC 3081

The CR indicates the presence of a PL/YS component contributing with $\approx 25\%$ of the flux at $\lambda 4020\text{\AA}$. The near-UV W's and overall spectrum are also well reproduced by the above combination (Fig. 14b). HOBL are not detected. NeIII λ 3968 + H ϵ emission can be observed filling the CaII H + H ϵ absorption.

4.2.3. Mrk 348

CR is 0.72 for this galaxy, thus indicating the presence of a PL/YS component contributing with 30% in flux at $\lambda 4020\text{\AA}$, and in approximate agreement with the W values. Fig. 14c shows also that the overall spectrum is well reproduced by this combination, taking into account that there is some emission in H9 and probably also in H10, making it impossible to detect the HOBL in absorption, if any. NeIII λ 3968 + H ϵ emission completely dominates over the CaII H + H ϵ absorption.

4.2.4. *Mrk 573*

H9 is filled by emission. The CR indicates the presence of a PL/YS component contributing with $\approx 20\%$ in flux at $\lambda 4020\text{\AA}$. The other two W's and overall continuum are also well reproduced by this combination (Fig. 14d). The small discrepancy in the CaII K line profile is explained as for the radio-galaxies above. HOBL are not detected. NeIII $\lambda 3968$ + H ϵ emission completely dominates over the CaII H + H ϵ absorption.

4.2.5. *IRAS 11215-2806*

This galaxy shows significant dilution in the near-UV W's, with the CaII K line profile better reproduced by a combination of a bulge plus 20% mass contribution of a 1 Gyr component – an additional model we had to construct increasing the contribution of the intermediate age population to fit the spectrum of this galaxy (Fig. 14e). The HOBL can be identified. There is some contamination of the CaII H + H ϵ absorption by NeIII $\lambda 3968$ + H ϵ emission.

4.2.6. *Fairall 316*

The W values are very similar to those of the old bulge template, and Fig. 14f shows that the latter is indeed a good representation of the nuclear spectrum of this galaxy. There is some contamination of the CaII H + H ϵ absorption by NeIII $\lambda 3968$ + H ϵ emission.

4.2.7. *ESO 417-G6*

The near-UV W's, CR and overall spectrum of this galaxy are best reproduced by the combination of a bulge template plus 10% mass contribution of a 1 Gyr stellar population

(Fig. 14g). The HOBL are at the detection limit, but can be identified because there seems to be no contamination by H9 and H10 emission. There is some contamination of the CaIIH + H ϵ absorption by NeIII λ 3968 + H ϵ emission.

In summary, of the seven nuclear spectra of S0 Seyfert’s 2, two can be reproduced by a bulge stellar population and three are better reproduced by a combination of the bulge template with the PL/YS component. The HOBL signatures can be observed in IRAS 11215-2806 and ESO 417-G6 due to a large contribution of an intermediate age 1 Gyr stellar population.

4.3. Sa

4.3.1. *Mrk 1210*

CR is 0.83 for this galaxy suggesting a PL/YS component contributing with $\approx 50\%$ of the flux at $\lambda 4020$, which is in agreement with the value obtained from W_{CaIIK} . The other two W values are contaminated by emission lines, which precludes the detection of the HOBL. Storchi-Bergmann et al. (1998) have shown that the extranuclear spectrum is dominated by an intermediate age population, which can be represented by our combination of a bulge plus 1% mass contribution of a 500 Myr stellar population. They have also shown that the nuclear spectrum could be well reproduced by the latter population plus a very young starburst, as evidenced by the Wolf-Rayet features (Storchi-Bergmann et al. 1998, Cid Fernandes et al. 1999). We have then constructed a model combining 70% in flux at $\lambda 4020$ of the extranuclear population plus 30% of the 3 Myr population to represent the nuclear spectrum of this galaxy, which is shown together with the observed nuclear spectrum in Fig. 15a.

The emission-lines in the nuclear spectrum are stronger than in the model, indicating

that the observations are consistent with the contribution of a 3 Myr stellar population but suggesting also that another source of continuum – the AGN continuum, is necessary to ionize the gas.

4.3.2. *CGCG 420-015*

The near-UV spectrum is best reproduced by a mixture of bulge plus 10% in mass of an intermediate age (1 Gyr) stellar population (Fig. 15b). The spectrum is somewhat noisy in the region, which together with some contamination by emission lines makes difficult the identification of the HOBL.

4.3.3. *IC 1816*

The CR of 0.66 suggests $\approx 15\%$ contribution of a PL/YS continuum. The W's suggest additional dilution which can be provided by an intermediate age population. We thus show in Fig. 15c two models: the bulge plus 15% flux contribution at $\lambda 4020$ of the PL/YS component, and the improved fit provided by combining the bulge with 10% in mass of a 1 Gyr stellar population before the combination with the PL/YS. The strong emission precludes a firm identification of HOBL.

4.3.4. *ESO362-G8*

The nuclear spectrum of this galaxy unambiguously shows all HOBL in absorption. The near-UV W's are well reproduced by the bulge template combined with 10% mass contribution of a stellar population with age between 100 and 500 Myrs, with the metal lines of the Seyfert 2 galaxy somewhat deeper most probably because of the lower metallicity

of the star clusters used to construct the young stellar templates. The CR measured for this galaxy was 0.35, much lower than the lowest template value (0.55), suggesting that the continuum was still reddened. We have thus corrected the continuum of this galaxy by an additional $E(B-V)=1$, which brought the CR value to 0.52 (about the minimum obtained for the sample), in agreement with the model selected from the W's (Fig. 15d). This very high reddening is consistent with the dust lane observed crossing the nuclear region (e.g. Malkan et al. 1998), and is in agreement with the $E(B-V)$ values obtained from emission lines (Fraquelli, Storch-Bergmann & Binette 2000).

In summary, among the 4 Sa's, there is one unambiguous case of a relatively evolved nuclear starburst, ESO 362-G8, clearly showing the HOBL in absorption. In addition, Mrk 1210 has a very young burst, for which the HOBL are filled with emission. For CGCG 420-015, and IC 1816 there is some contribution of intermediate age population and for the latter, there is also evidence of a PL/YS continuum.

4.4. Sab, Sb and Sbc

4.4.1. NGC 1386

The W's, CR and spectrum are best reproduced by the bulge template plus 10% im mass of a 1 Gyr population. This fit is shown in Fig. 16a, where the the HOBL can be observed. The $NeIII\lambda 3968 + H\epsilon$ emission are almost filling the $CaIIH + H\epsilon$ absorption.

4.4.2. NGC 6890

The CR of 0.7 indicates the presence of a PL/YS continuum contributing with $\approx 30\%$ to the flux at $\lambda 4020$, in agreement also with the W values. Some contribution of an

intermediate population is also possible, and a model including 10% mass contribution of a 1 Gyr stellar population, combined with 20% in flux of a PL gives a slightly improved fit in the H9–H10 region, as shown in Fig. 16b. $\text{NeIII}\lambda 3968 + \text{He}\epsilon$ emission are filling the $\text{CaIIH} + \text{He}\epsilon$ absorption.

4.4.3. *NGC 7582*

This galaxy is well known from the emission-lines (diagnostic diagrams) to present a composite Seyfert 2 + Starburst spectrum. The HOBL are easily seen (Fig. 16c). The near-UV W's, CR and spectral distribution are well represented by a bulge template plus 1% mass contribution of a 50 Myr stellar population. Again, we attribute the poor fit of the CaIIK line mostly to the lower metallicity of the young templates as compared to the nuclear region of the galaxy. There is contamination of the $\text{CaIIH} + \text{He}\epsilon$ absorption by $\text{NeIII}\lambda 3968 + \text{He}\epsilon$ emission.

4.4.4. *Mrk 607*

The near-UV W's, CR and spectrum are best reproduced by a bulge plus 10% mass contribution of a 1 Gyr stellar population (Fig. 16d). The spectrum is somewhat noisy in the region, and thus the HOBL cannot be unambiguously identified. $\text{NeIII}\lambda 3968 + \text{He}\epsilon$ emission are filling the $\text{CaIIH} + \text{He}\epsilon$ absorption.

4.4.5. *MCG-05-27-013*

CR is 0.7 for this galaxy suggesting a 20% contribution of a PL/YS component. The spectrum is dominated by line emission, including in the high order Balmer lines and the

blue end of the spectrum is noisy. It is not possible to identify the HOBL in absorption (Fig. 16e).

In summary, for the five Sab, Sb and Sbc's, NGC 7582 presents the HOBL signatures of a nuclear starburst, NGC 1386, Mrk 607 and possibly also NGC 6890 have 10% contribution in mass of intermediate age 1 Gyr stars and the CR of MCG-05-27-013 and NGC 6890 suggest the presence of a PL/YS component contributing with 20% in flux at $\lambda 4020\text{\AA}$.

4.5. Sc and Sd

4.5.1. NGC 5135

The HOBL are clear in the spectrum. The W's, CR and other features of the spectrum can be approximately reproduced by the combination of 50% each in flux at $\lambda 4020$ of two of our models: the first is the bulge template combined with 1% in mass of a 10 Myrs stellar population, and the second is the bulge template combined with 1% in mass of a 100 Myrs stellar population (Fig. 17a). There is some line emission of $\text{H}\epsilon + \text{NeIII}\lambda 3968$, H8 and possibly H9.

The starburst in this galaxy has been extensively studied by González Delgado et al. (1998) and González Delgado, Heckman & Leitherer (2000), hereafter GD98 and GD00. GD98 have shown that the UV spectrum presents clear signatures of O and B stars, estimating an age between 3 and 5 Myr for the burst, while GD00 concluded that there is also a similar contribution in flux from an intermediate age population and a small contribution of an old component. Our model is consistent with the latter mixture.

4.5.2. *NGC 5643*

The near-UV W's, CR and spectrum can be best reproduced by the combination of the bulge template plus 1% in mass of a 100 Myr stellar population, except for the Ca II K line, mostly due to the lower metallicity of the young template, as discussed previously. The HOBL can be identified (Fig. 17b). NeIII λ 3968 + H ϵ emission are almost filling the CaIIH + H ϵ absorption.

4.5.3. *NGC 6300*

The near-UV W's, CR and spectral distribution are best reproduced by a mixture of a bulge template plus 10% mass contribution of a 1 Gyr stellar population. The model is compared with the data in Fig. 17c, where the HOBL are at the limit of detection.

4.5.4. *NGC 7130*

Fig 17d shows the clear HOBL in this spectrum, another case of nuclear starburst well studied by GD98 and GD00. The latter authors have suggested the same population as that derived for NGC 5135. Although the W's support the same population, the bluer continuum of NGC 7130 suggests a somewhat younger population, or a mixture including a larger proportion of the younger components. The model we show in the figure is the same composite model as the one adopted for NGC 5135, with a somewhat larger contribution in flux at λ 4020 of the bulge combined with the 10 Myr stellar population: 75%, while the bulge combined with the 100 Myr population contributes with 25% of the flux.

In summary, for the 4 Sc and Sd Seyfert's, three present recent episodes of star formation in the nuclear region, with the HOBL clearly visible in the spectra, while one

presents $\approx 10\%$ mass contribution of an intermediate age population.

5. Comparison with other works

The above results can be compared with those from the synthesis of SSC99. There is good agreement for most galaxies for which the HOBL are observed in the spectra: the young components in our simple models coincide, approximately, with the dominant young components obtained by SSC99. One systematic difference seems to be the contribution of the intermediate age components, found to be present in most cases by SSC99, but only in approximately half of the sample here. We attribute this difference to two factors: (1) the models of SSC99 were not as strongly constrained in the blue end of the spectrum as in the present work, providing an optimized representation of the data over the spectral range $\lambda\lambda 3700\text{--}7000\text{\AA}$; (2) the lower metallicity of some of the star clusters used to construct the 1 Gyr template, which is a mixture of spectra of LMC and Milky Way disk clusters, while the synthesis performed by SSC99 is based on a grid of parameters including the high metallicity end.

González Delgado et al. (2000, GD00) have recently finished a similar spectral study in which they investigate the age of the stellar population at and around the nucleus of a sample of (also) 20 Seyfert 2 galaxies. They cover the spectral region $\lambda\lambda 3700\text{--}4400\text{\AA}$ at a similar spectral resolution to our observed spectra, but using models with the same resolution. This better resolution in the modeling allows the detection of the He I absorption (e.g. $\lambda\lambda 3819, 4387$ and 4922) in some cases, providing a better dating of the starbursts. The higher spectral resolution also allows a more precise evaluation of the emission-line contamination in the high order Balmer lines.

GD00 find signatures of recent star formation in the nuclear spectrum of 6 galaxies

plus 3 or 4 cases in which these signatures are found once the nebular Balmer emission lines are subtracted. In two other cases they find significant contribution of intermediate age stars. There are 5 galaxies in the sample of GD00 in common with the present study: Mrk 348, Mrk 573, NGC 1386, NGC 5135 and NGC 7130. Similarly to what we have found, they conclude that Mrk 348, Mrk 573 and NGC 1386 have a dominant old stellar population, and that the near-UV nuclear spectrum of NGC 5135 and NGC 7130 is dominated by light from young and intermediate age stars.

6. The nature of the PL/YS continuum

As pointed out above, there is a degeneracy between the power-law and starburst continua for ages ≤ 10 Myrs. This occurs for mass contributions of the young component much smaller than those in the models of Fig. 6: for example, for a typical 30% flux contribution of PL/YS at $\lambda 4020\text{\AA}$, if it is due to the continuum of a 10 Myr stellar population, the corresponding mass contribution is only $\approx 0.015\%$ that of the bulge. This degeneracy is illustrated in Fig. 18, where we plot the combined spectrum of a bulge and a PL contributing with 20% and 40% in flux at $\lambda 4020\text{\AA}$, together with the combined spectra of the bulge and a 10 Myr star cluster template, for the same proportions in flux as the PL, and with the combined spectrum of the bulge and a 3 Myr star cluster contributing in flux with half the proportions above, namely 10% and 20%. A young starburst in nature will most probably present a spread in age, and the spectral distribution will probably be more similar to a combination of the 3 and 10 Myr templates.

It can be observed that, for $\lambda \geq 3500\text{\AA}$, the combination with a PL can hardly be distinguished from that with the young burst templates if their contribution to the flux is 20%. The only constraint here could be the strength of the emission lines.

Figure 18 shows that contributions in flux $\geq 40\%$ at $\lambda 4020\text{\AA}$ and good signal-to-noise (S/N) ratio spectra are necessary to allow the distinction between a featureless PL and a young starburst in terms of continuum features, such as the HOBL. Additional constraints could be the emission-line strengths and the UV spectrum slope. The UV spectrum can be observed rising much more steeply for the 10 Myr stellar population than for the PL. Unfortunately our data do not extend enough to the UV to allow the use of this constraint.

In our sample, the PL/YS contribution is always smaller than or equal to 30%, and it is thus not possible to determine its origin from the near-UV features alone. In Storchi-Bergmann et al. (1998), we have discussed the origin of the near-UV continuum of Mrk 348 and Mrk 573: in the former, from the work of Tran (1995a,b,c), $\approx 10\%$ of the flux is due to scattered light, and thus the remainder could be due to young stars. Population synthesis has indeed shown that a mixture of a 10 Myr and a 3 Myr stellar population can reproduce the continuum. In Mrk 573, at least part of the blue continuum is also due to scattered light, as revealed by the images of Pogge & De Robertis (1993), but we have no constraint on its value.

The only constraint we could try to use here is the strength of the emission-lines; for example, if the near-UV continuum were entirely due to a very young starburst (the 3 Myr one), the equivalent widths W_{em} 's of the Balmer emission lines in the nuclear spectra should be similar to that of the model combining the bulge and the 3 Myr template. Most frequent in nature is however the case in which there is some spread in age for the starburst so that the blue continuum is also due to non-ionizing (ageing) blue stars, and the W_{em} 's should then be smaller than in the simple model with the 3 Myr template.

We have measured the equivalent width $W_{H\beta}$ of the nuclear $H\beta$ emission line and found that it was smaller than in the simple model above for the 2 radio galaxies PKS 0349-27, PKS 0634-20 and for NGC 6890, and about the same order for NGC 3081. In all other cases

– 3C 33, Mrk 348, Mrk 573, and MCG 05-27-13, the observed nuclear $W_{H\beta}$ ’s are larger than in the model. We can thus conclude that, if a starburst is the origin of the blue continuum in the above galaxies, it is an ageing one ($\text{age} \geq 10 \text{ Myr}$) for the first three above, and could be a very young ($\approx 3 \text{ Myr}$) in the other cases. But we also remark that, although the blue continuum could be due to young stars, the emission-line ratios in all cases (and even the W ’s in the last three cases) require additional ionizing sources – in other words, the starburst continuum cannot account alone for the emission-line ratios (and emission-line luminosities in the last three cases).

7. Comparison with “normal” galaxies of the same Hubble type

A comparison can be made between the near-UV properties of the Seyfert’s above and non-Seyfert’s of the same Hubble type. Using the CaIIK W ’s values from Bica & Alloin (1987) as representative of a sample of normal galaxies, we obtain the following typical values, calculated as averages from approximately 30 galaxies of each Hubble type: (i) for Sa’s, $W_{\text{CaIIK}} = 16.5 \pm 1.6 \text{ \AA}$; (ii) for Sb’s, $W_{\text{CaIIK}} = 13.8 \pm 4.2 \text{ \AA}$ and (iii) for Sc’s, $W_{\text{CaIIK}} = 9.9 \pm 4.9 \text{ \AA}$. Note that for later types, the spread of W ’s increases, simply reflecting the variety of mixtures of old (bulge) stellar population and star-forming events in the central region of these galaxies. For ellipticals and S0’s, similar values to those of Sa galaxies are obtained.

From the 20 Seyfert’s, 11 are early-type galaxies, classified as S0 or Sa; in NGC 1358 and Fairall 316, W_{CaIIK} is typical of early-type galaxies; in the other 9, the W ’s are smaller, indicating the need of a blue continuum. This blue continuum is clearly due to recent ($\text{age} < 500 \text{ Myr}$) enhanced star-formation in ESO 362-G8 and in Mrk 1210, and to intermediate age stars in IRAS 11215-2806, and ESO 417-G6. For Mrk 348, Mrk 573 and NGC 3081, a PL/YS component is favored. This component is at least partially due to scattered light

observed as polarized light in Mrk 348 and Mrk 573, but the unpolarized flux could be partially originated in the continuum of a nuclear starburst younger than 10 Myr.

Nine sample galaxies have later Hubble types, from Sb to Sd. Contrarily to the earlier types, the W_{CaIIK} values are within the range observed for non-Seyfert's. Four of these galaxies present recent (age <500 Myr) episodes of star-formation in the nuclei as revealed by the HOBL in NGC 7582, NGC 5643, NGC 5135 and NGC 7130. NGC 1386, NGC 6300 and Mrk 607 are cases in which there is enhanced contribution of an intermediate age population of ≈ 1 Gyr. MCG 5-27-13 and NGC 6890 are cases in which a PL/YS is necessary.

In summary, recent star formation episodes have been found in the nuclei of 2 of the 11 early type Seyfert's and 4 of the 9 late type Seyfert's, showing a tendency of these episodes to be found more frequently in late-type Seyfert's.

8. Summary and Conclusions

We have constructed models combining spectral distributions of a typical bulge plus a young stellar population template in the spectral range $\lambda\lambda 3600\text{-}4100\text{\AA}$ in order to investigate the detectability of recent star-formation episodes in the nuclear region of Seyfert galaxies, which usually have prominent bulges.

The high order Balmer lines (HOBL) are good indicators of the presence of young to intermediate age populations as far as the mass contribution of these young components, as compared with the bulge mass, is larger than 1% for ages of ≈ 100 Myr, or larger than $\approx 0.1\%$ for ages of ≈ 10 Myr. We conclude in addition that the continuum ratio $CR = \lambda 3660 / \lambda 4020$ is an important discriminator of very young stellar populations, as its value can only be larger than $CR = 0.6$ for models including stellar populations younger than 50 Myr. If the flux contribution at $\lambda 4020$ of these very young populations is smaller than 40% (corresponding

to 0.02% of the mass of the bulge for the 10 Myr template), it is not possible to distinguish its spectral signatures (e.g., the HOBL) from a featureless power-law. Thus, the problem of degeneracy between the featureless AGN continuum and the continuum of a stellar population of 10 Myr or younger still remains at the above flux levels.

By comparing the nuclear spectrum of a sample of 20 Seyfert 2's and 3 radio-galaxies with the models above, signatures of recent to intermediate age star-formation in the form of high-order Balmer absorption lines (HOBL) have been found in 9 Seyfert 2's. From previous analyses of the emission-line features, enhanced recent star-formation has been found also in Mrk 1210. In summary, half of our Seyfert 2 sample show signatures of young to intermediate stars. In six cases (30% of the sample), the starburst is younger than 500 Myrs: ESO 362-G8, NGC 7582, NGC 5135, NGC 5643 and NGC 7130. In the cases of ESO 417-G6, IRAS 11215-2806 NGC 1386 and NGC 6300 the HOBL are due to a large contribution of intermediate age (1 Gyr) stars. Intermediate age stars seem to contribute also to the nuclear spectrum of IC 1816, NGC 6890 and the radio galaxy 3C33.

The incidence of recent star formation seems to be related to the Hubble type in our sample of 20 Seyfert 2's: signatures from young components with ages <500 Myr have been found in 4 of the 9 late-type galaxies, but only in 2 of the 11 early-type galaxies. This tendency seems to be present also in the sample of González Delgado et al. (1999).

For the remaining 5 late-type galaxies, two appear to present a PL continuum (alternatively due to stellar populations younger than 10 Myr) and three present an intermediate age (1 Gyr) component.

Out of the nine early-type galaxies without recent central star-formation, the stellar population is well reproduced by the bulge template in two of them, by the bulge plus 10% contribution in mass of an intermediate population in other three, while in the remaining four, a power-law seems to be necessary. The nature of the latter component requires further

investigation, due to its degeneracy with very young (≤ 10 Myr) stellar population spectra in the wavelength range investigated here. If such component were due to very young stars in all cases, then the number of Seyfert 2 with significant contribution from young stars to the nuclear spectra would increase to 12 (60%), in our sample of 20 Seyfert 2's.

It is essential to continue the present investigation along two lines: (1) assess the statistical significance of our findings observing a larger and well defined sample of Seyfert 2's, together with a comparison sample of normal galaxies of the same Hubble types; (2) investigate the nature of the power-law continuum. The degeneracy of this continuum with those from very young stellar populations could be raised, in principle, in the UV spectral region.

We thank the referee, Rosa González Delgado, for many suggestions which improved the paper. This work has benefited also from discussions with Roberto Cid Fernandes, Henrique Schmitt and Tim Heckman. We thank the support from the brazilian institutions CNPq, CAPES and FAPERGS.

REFERENCES

- Bica, E. & Alloin, D. 1986, A&A, 162, 21
- Bica, E. & Alloin, D. 1987, A&AS, 70, 281
- Bica, E., Alloin, D. & Schmidt, A. 1990, MNRAS, 242, 241
- Bica, E., Alloin, D. & Schmitt, H. R. 1994, A&A, 283, 805
- Cid Fernandes, R. & Terlevich, R. 1992, in *Relationships between Active Galactic Nuclei and Starbursts Galaxies*, ASP Conf. Ser., 31, Astron. Soc. Pac. (San Francisco)
- Cid Fernandes, R. & Terlevich, R. 1995, MNRAS, 272, 423
- Cid Fernandes, R., Schmitt, H. R. & Storchi-Bergmann, T. 1998, MNRAS, 297, 579
- Cid Fernandes, R., Lacerda, R. R., Schmitt, H. R. & Storchi-Bergmann, T. 1999, IAU Symp. 193, eds. K. A. van der Hucht, G. Koenigsberger & P. R. J. Enens, ASP, p.590
- de Vaucouleurs, G. et al. 1991, Third Reference Catalog of Bright Galaxies (RC3), New York: Springer
- Fraquelli, H. A., Storchi-Bergmann, T. & Binette, L. 2000, ApJ, 532, 867
- González Delgado, R. M., Heckman, T. M. & Leitherer, C. 2000, in press
- González Delgado, R. M., Leitherer, C. & Heckman, T. M. 1999, ApJS, 125, 489
- González Delgado, R. M., Heckman, T., Leitherer, C., Meurer, G., Krolik, J., Wilson, A. S., Kinney, A. & Koratkar, A. 1998, ApJ, 505, 174
- Heckman, T., Krolik, J., Meurer, G., Calzetti, D., Kinney, A., Koratkar, A., Leitherer, C., Robert, C. & Wilson, A. S. 1995, ApJ, 452, 549
- Heckman, T. M., González Delgado, R., Leitherer, C., Meurer, G. R., Krolik, J., Wilson, A. S., Koratkar, A. & Kinney, A. 1997, ApJ, 482, 114 (H97)

- Leitherer, C. et al. 1996, PASP, 108, 996
- Malkan, M. A., Gorjian, V. & Tam, R. 1998, ApJS, 117, 25
- Norman, C. & Scoville, N. 1988, ApJ, 332, 124
- Perry, J. J. & Dyson, J. E. 1985, MNRAS, 213, 665
- Pogge, R. W. & De Robertis, M. M. 1993, ApJ, 404, 563
- Schmidt, A. A., Alloin, D. & Bica, E., 1995, MNRAS, 273, 945
- MNRAS, 278, 965
- Schmitt, H. R., Storchi-Bergmann, T. & Cid Fernandes, R. 1999, MNRAS, 304, 35
- Seaton, M J. 1979, MNRAS, 187, 73P
- Storchi-Bergmann, T., Bica, E., Kinney, A. L. & Bonatto, C. 1997 MNRAS, 290, 231
- Storchi-Bergmann, T., Cid Fernandes, R. & Schmitt, H. R. 1998, ApJ, 501, 94
- Storchi-Bergmann, T., Kinney, A. & Challis, P. 1995, ApJS, 98, 103
- Terlevich, E., Diaz, A. I. & Terlevich, R. 1990, MNRAS, 242, 271
- Tran, H. D. 1995a, ApJ, 440, 565
- Tran, H. D. 1995b, ApJ, 440, 578
- Tran, H. D. 1995c, ApJ, 440, 597

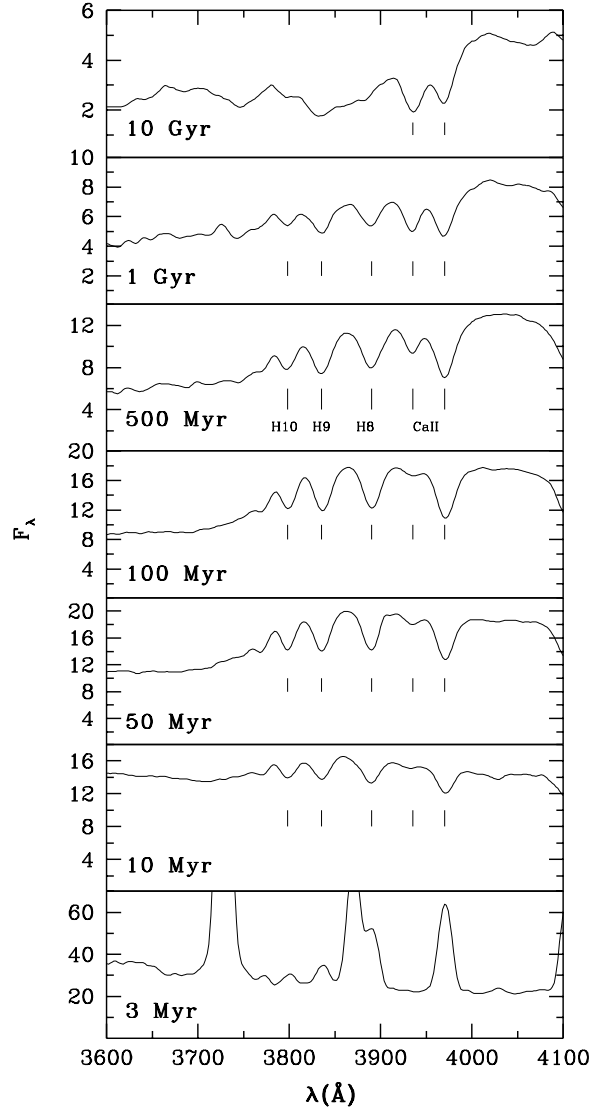


Fig. 1.— Stellar population templates, corresponding to ages from 3 Myr to 10 Gyr. The main absorption features are identified.

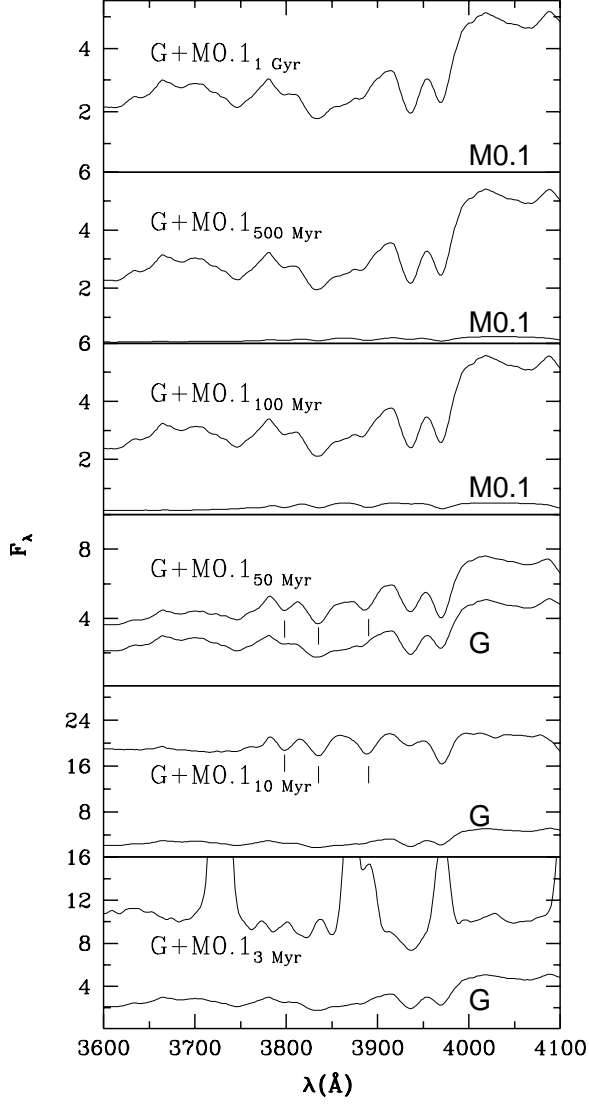


Fig. 2.— Top of each panel: Composite spectra constructed by combining a bulge template (G) plus 0.1% in mass (M) of bursts with ages from 3 Myr to 1 Gyr. Bottom of each panel: contribution of the component with less flux to the combined template.

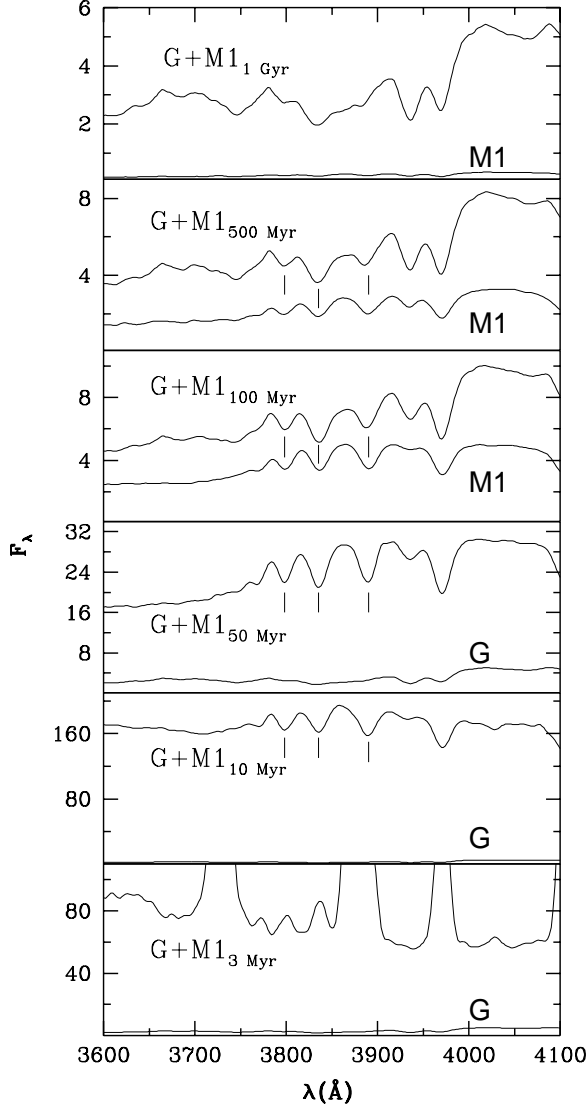


Fig. 3.— Top of each panel: Composite spectrum constructed by combining a bulge template (G) plus 1% in mass (M) of bursts with ages from 3 Myr to 1 Gyr. Bottom of each panel: contribution of the component with less flux to the combined template.

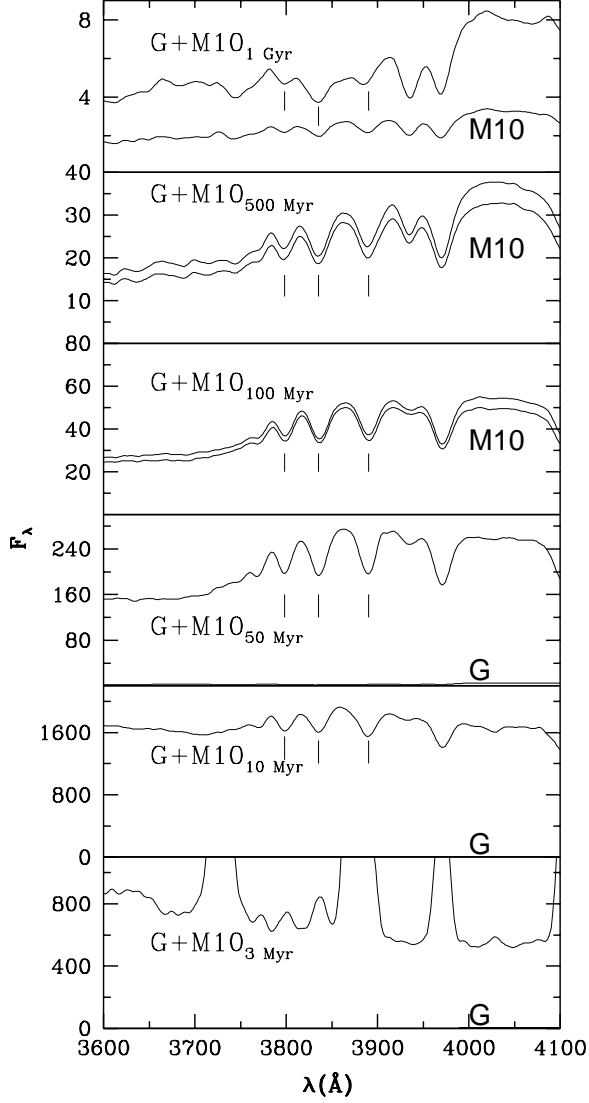


Fig. 4.— Top of each panel: Composite spectra constructed by combining a bulge template (G) plus 10% in mass (M) of bursts with ages from 3 Myr to 1 Gyr. Bottom of each panel: contribution of the component with less flux to the combined template.

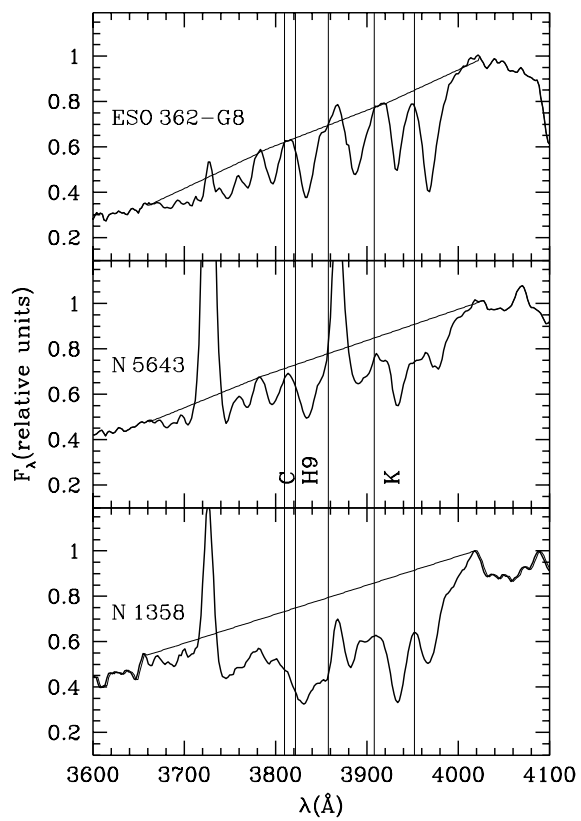


Fig. 5.— Illustration of the continuum and windows (vertical lines) used in the measurements of the equivalent widths W_C , W_{H9} and W_{CaK} for three Seyfert 2's of the sample.

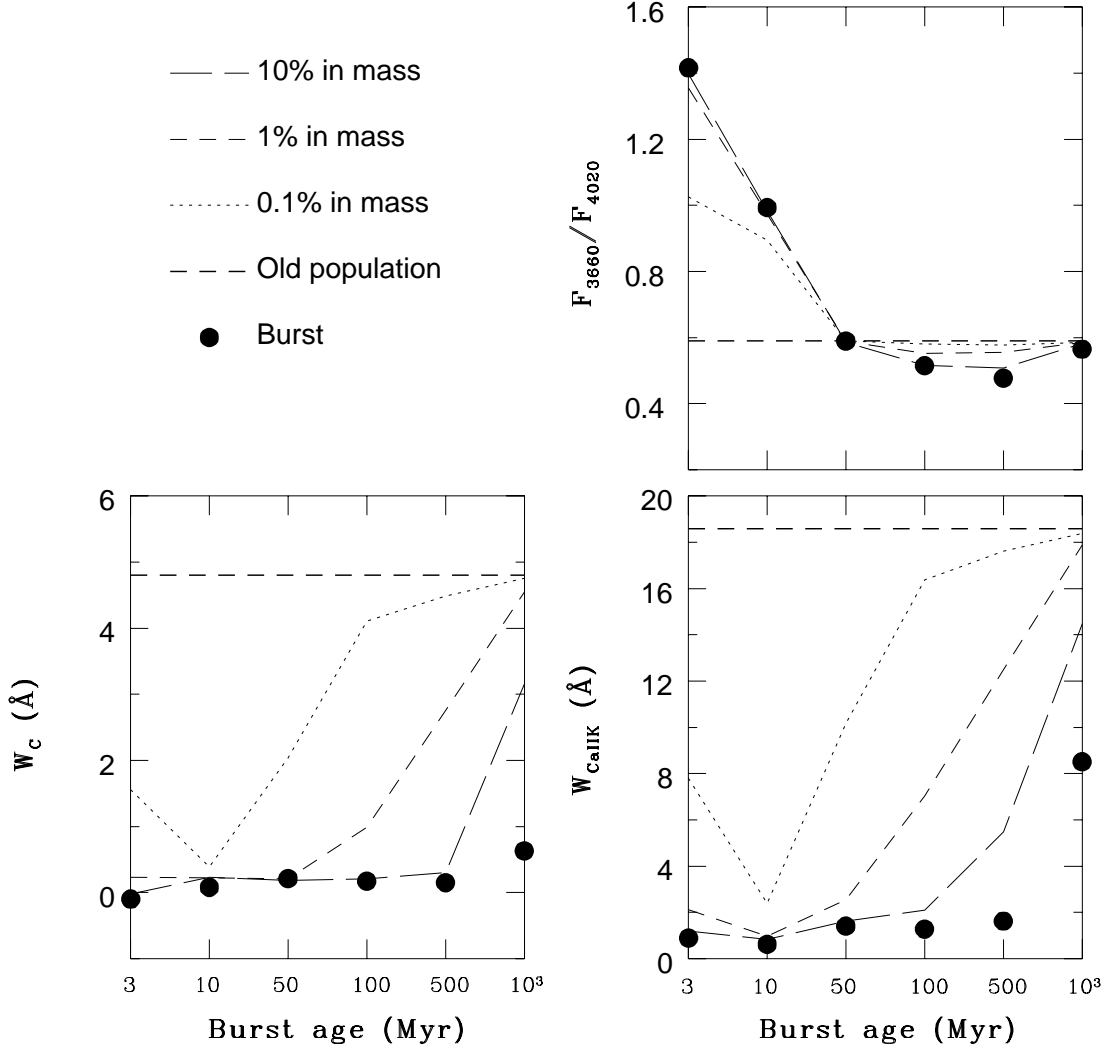


Fig. 6.— The continuum ratio $CR=F_{3660}/F_{4020}$ and equivalent widths W_C and W_{CaIIK} for synthetic spectra constructed combining a bulge template and bursts of varying ages contributing with zero (heavy dashed line), 0.1% (dotted line), 1%(dashed line), 10% (long-dashed) and 100% (filled circles) in mass.

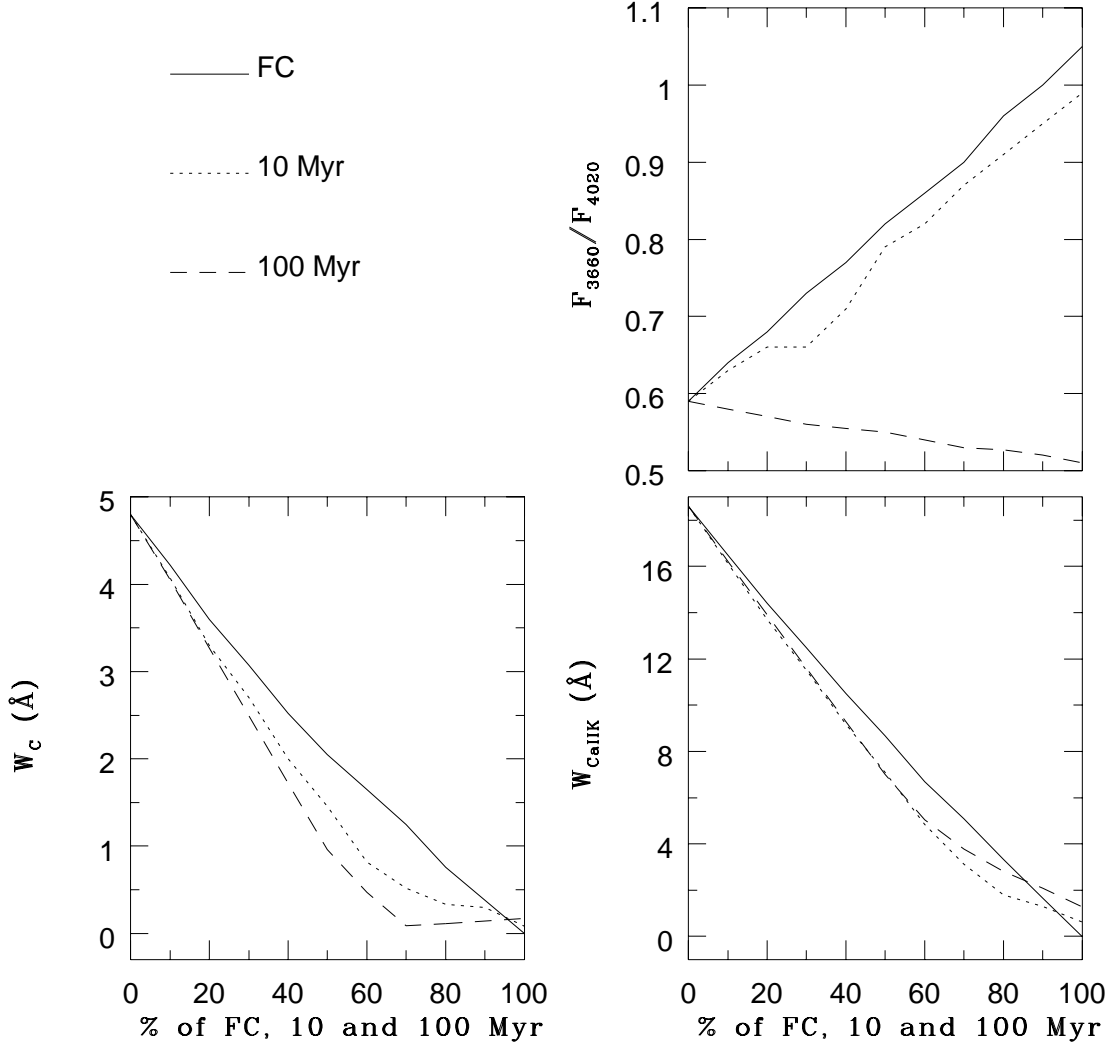


Fig. 7.— The continuum ratio $CR=F_{3660}/F_{4020}$ and equivalent widths W_C and W_{CaIIK} for synthetic spectra constructed combining a bulge template and increasing fractions (in flux at $\lambda 4020\text{\AA}$) of a PL (continuous line), a 10 Myr (dotted line) and a 100 Myr (dashed line) burst template.

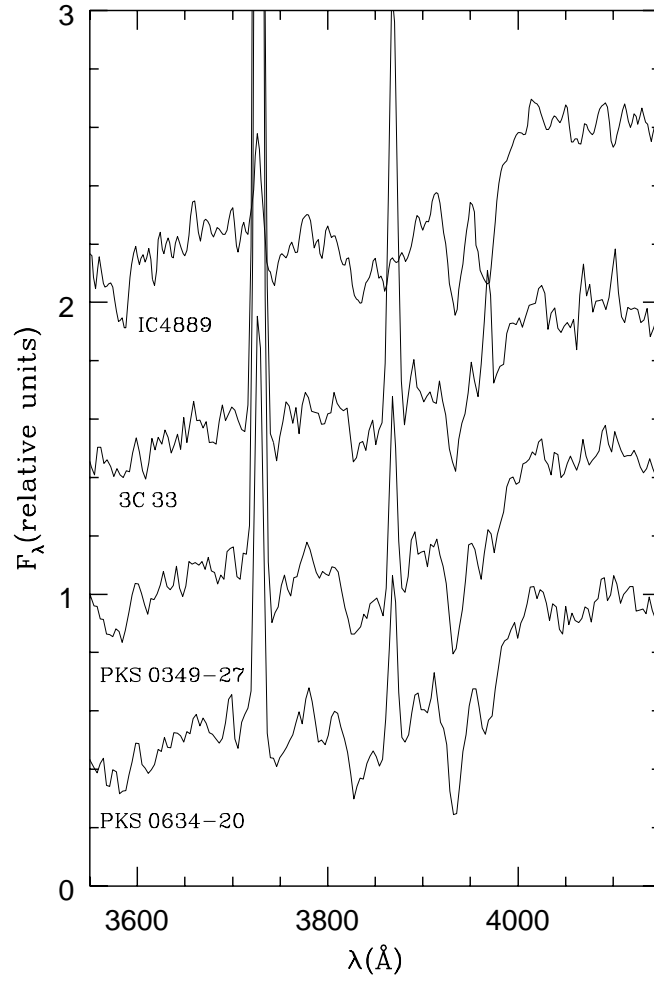


Fig. 8.— Spectra of the elliptical and three radio galaxies of the sample normalized at $\lambda 4020$ and shifted for clarity.

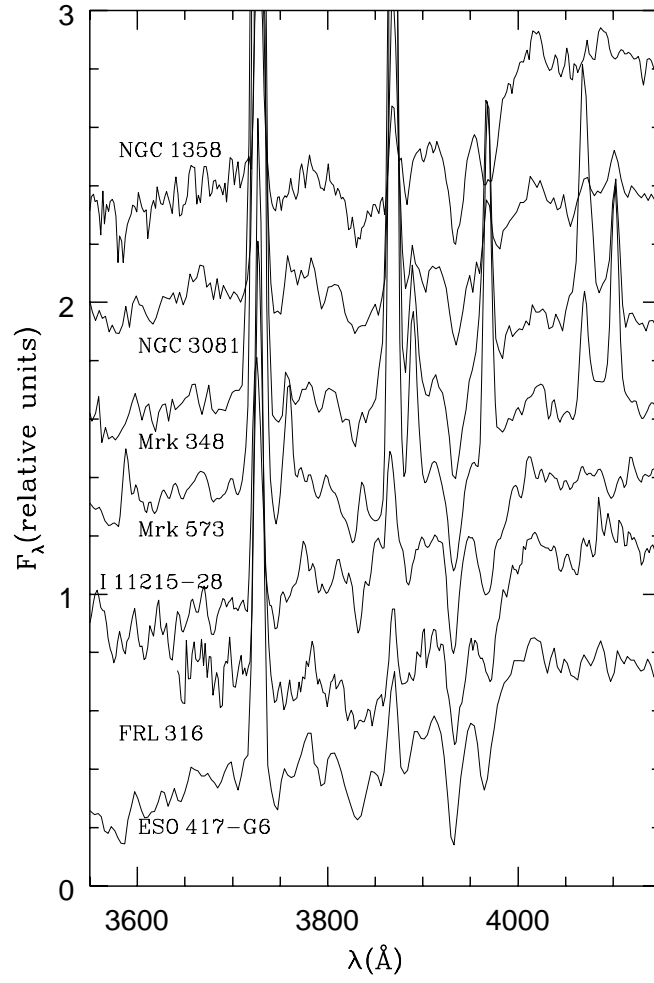


Fig. 9.— Spectra of the 7 S0 Seyfert 2 galaxies of the sample normalized at $\lambda 4020$ and shifted for clarity.

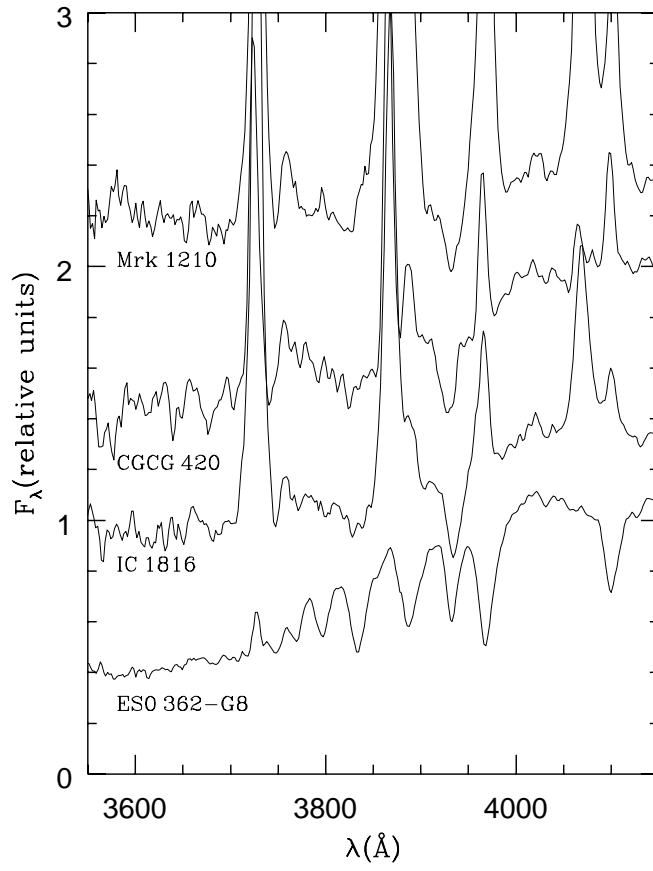


Fig. 10.— Spectra of the 4 Sa Seyfert 2 galaxies of the sample normalized at $\lambda 4020$ and shifted for clarity.

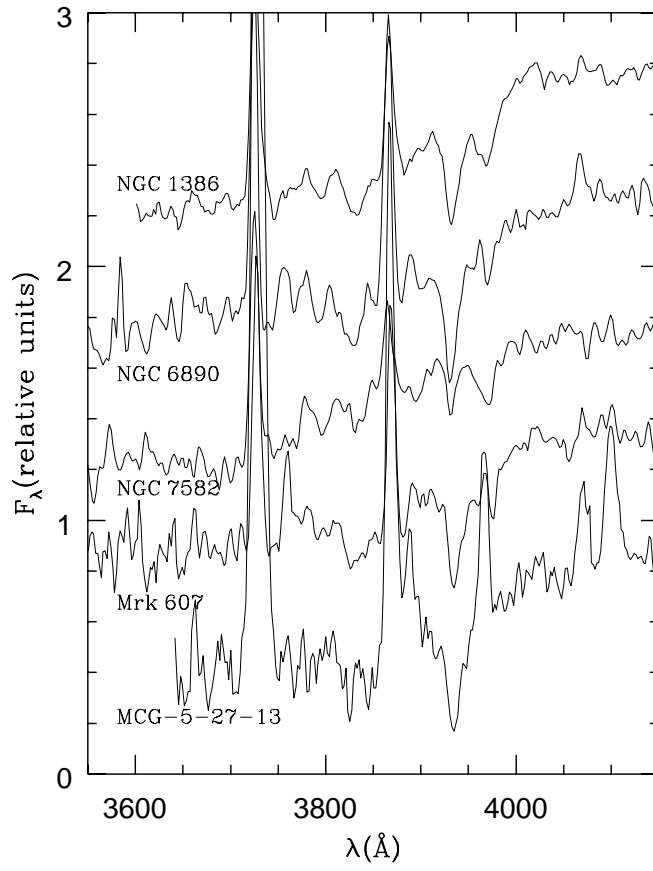


Fig. 11.— Spectra of the 5 Sb Seyfert 2 galaxies of the sample normalized at $\lambda 4020$ and shifted for clarity.

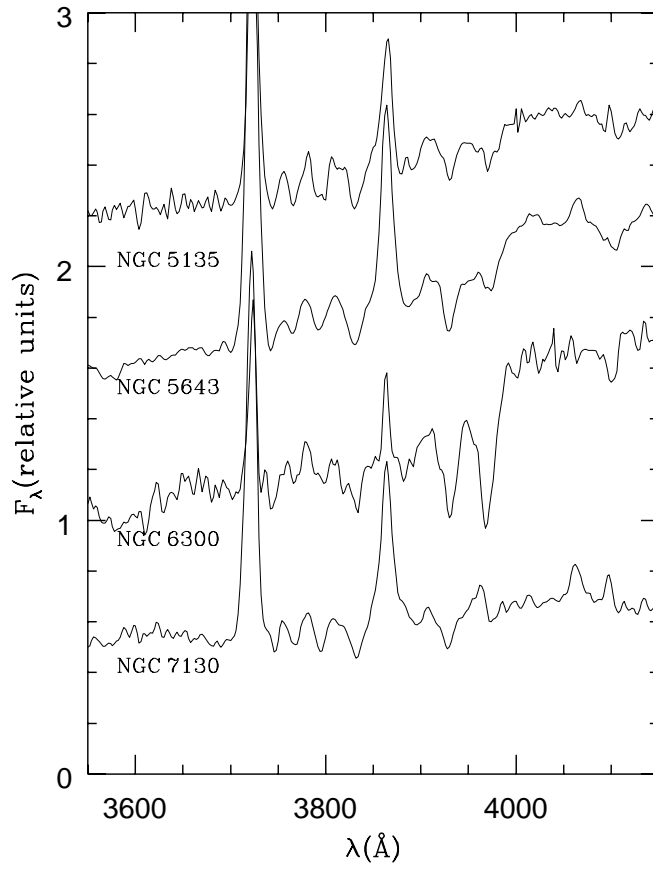


Fig. 12.— Spectra of the 4 Sc Seyfert 2 galaxies of the sample normalized at $\lambda 4020$ and shifted for clarity.

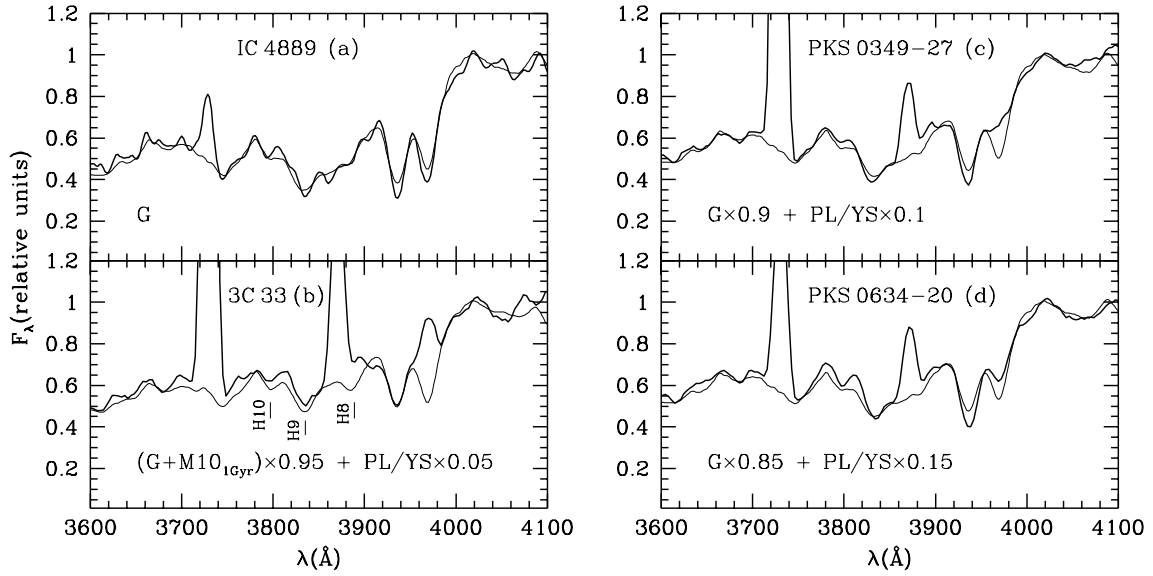


Fig. 13.— Comparison of the nuclear spectrum of the normal elliptical galaxy IC 4889 and the three radio ellipticals (heavy lines) with the best models (thin lines). Labels: G represents the bulge template, Mx_y represents a burst of age y contributing with $x\%$ (in mass) of the bulge mass and PL/YS is the power-law/young stars component. The high order Balmer lines H10, H9 and H8 (HOBL) are identified by vertical lines.

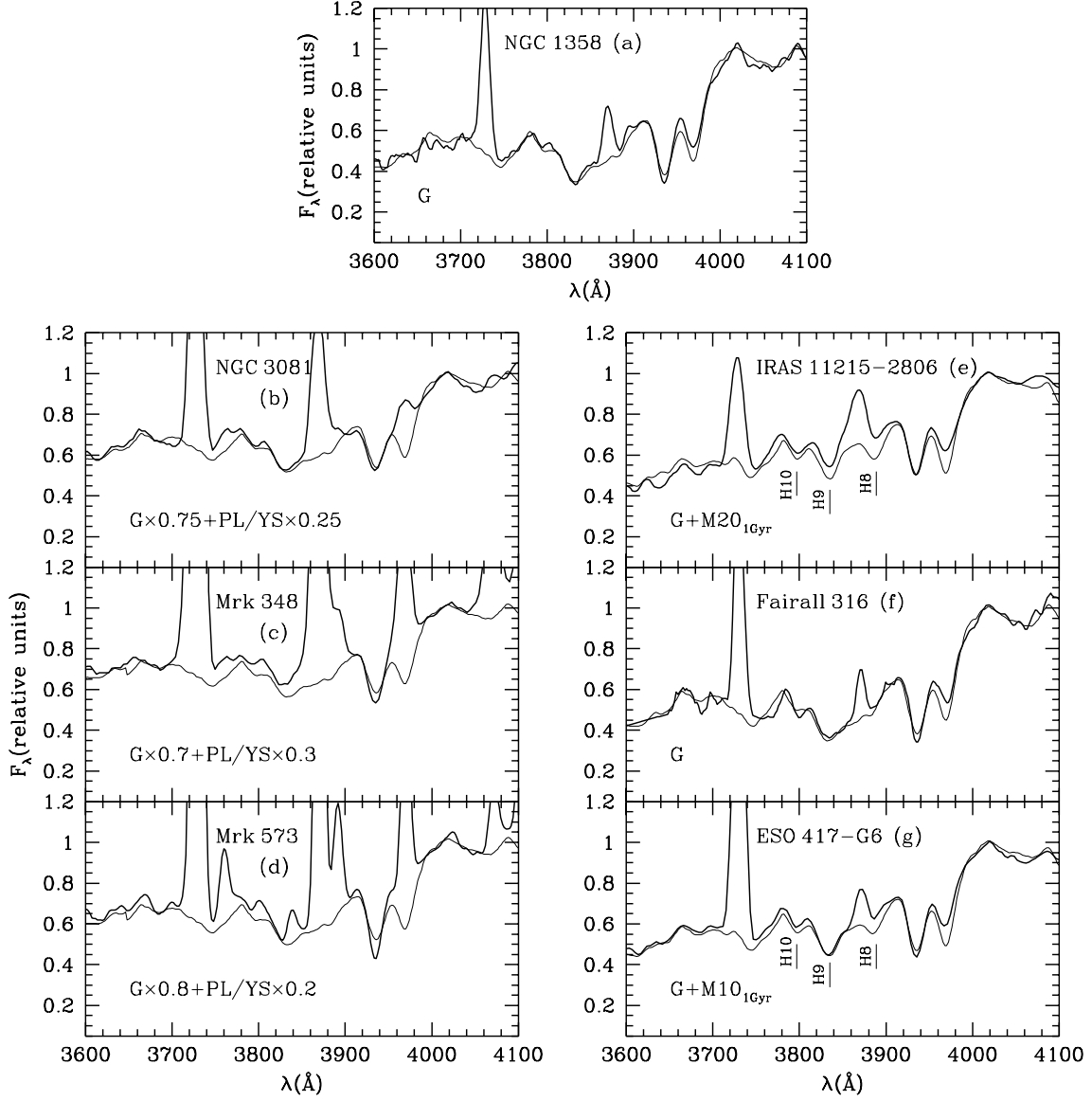


Fig. 14.— Comparison between the nuclear spectrum of the S0 Seyfert’s (heavy lines) and the best models (thin lines). Labels as in Fig.13. Models for Mrk 348 and Mrk 573 include the Balmer continuum from the emitting gas.

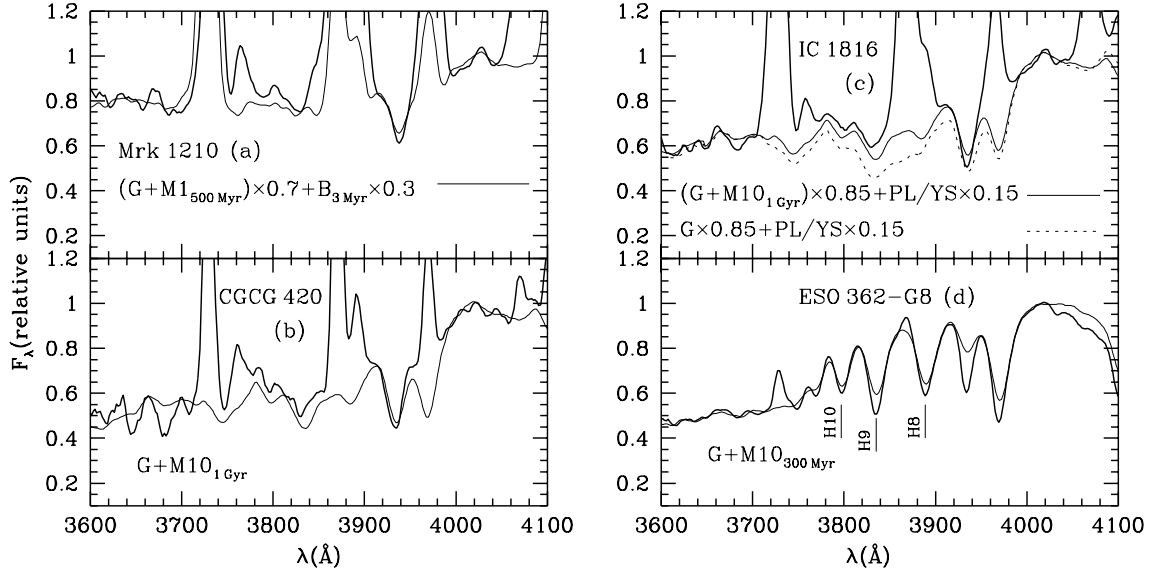


Fig. 15.— Comparison between the nuclear spectrum of the Sa Seyfert’s (heavy lines) and the best models (thin lines). Most labels as in Fig.13 with $B_{3\text{ Myr}}$ representing the 3 Myr burst. Models for Mrk 1210 and IC 1816 include the Balmer continuum from the emitting gas.

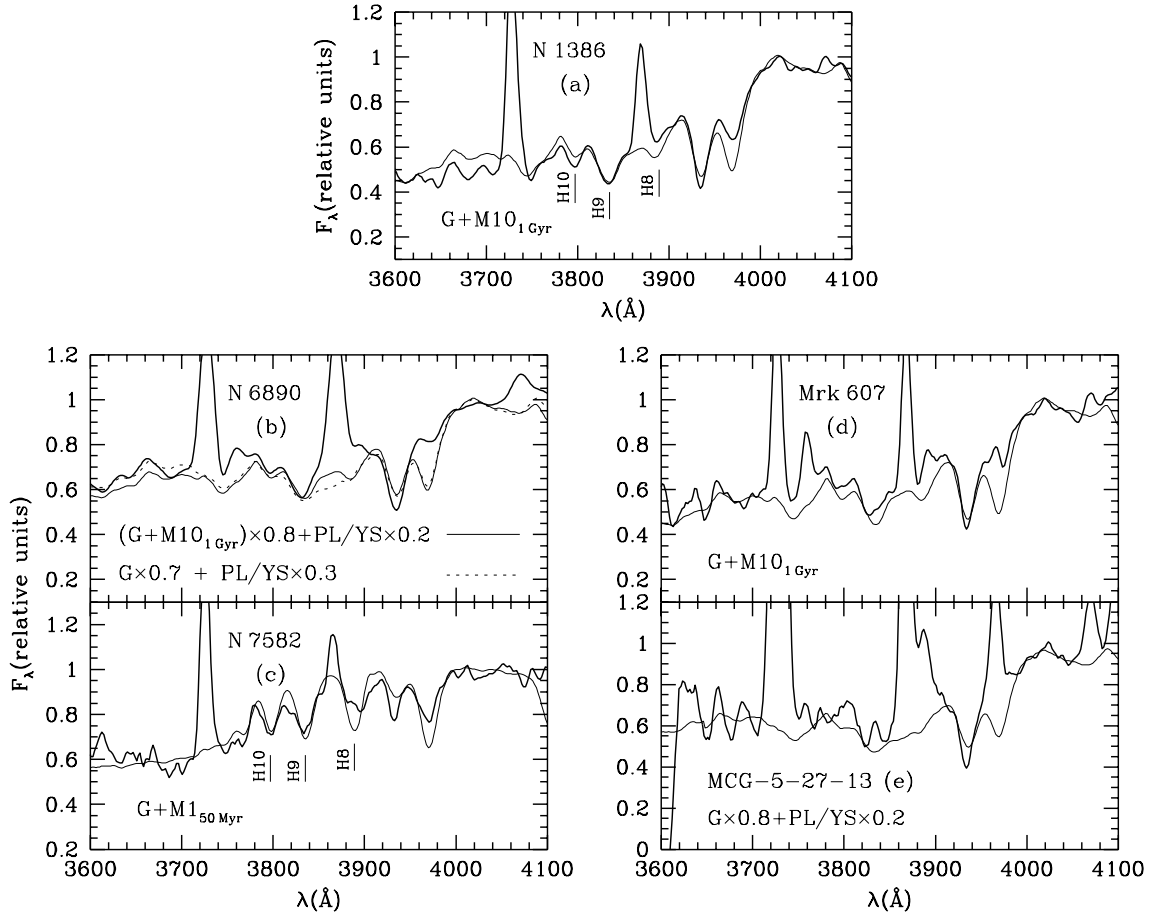


Fig. 16.— Comparison between the nuclear spectrum of the Sb Seyfert's (heavy lines) and the best models (thin lines). Labels as in Fig.13. Model for MCG-05-27-13 includes the Balmer continuum from the emitting gas.

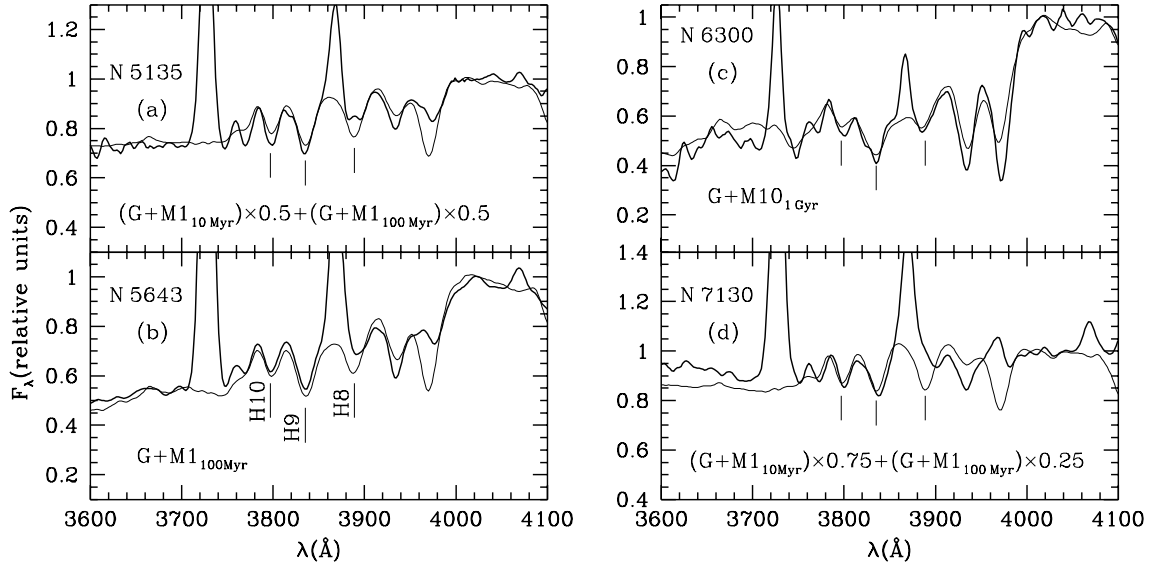


Fig. 17.— Comparison between the nuclear spectrum of the Sc Seyfert's (heavy lines) and the best models (thin lines). Labels as in Fig.13.

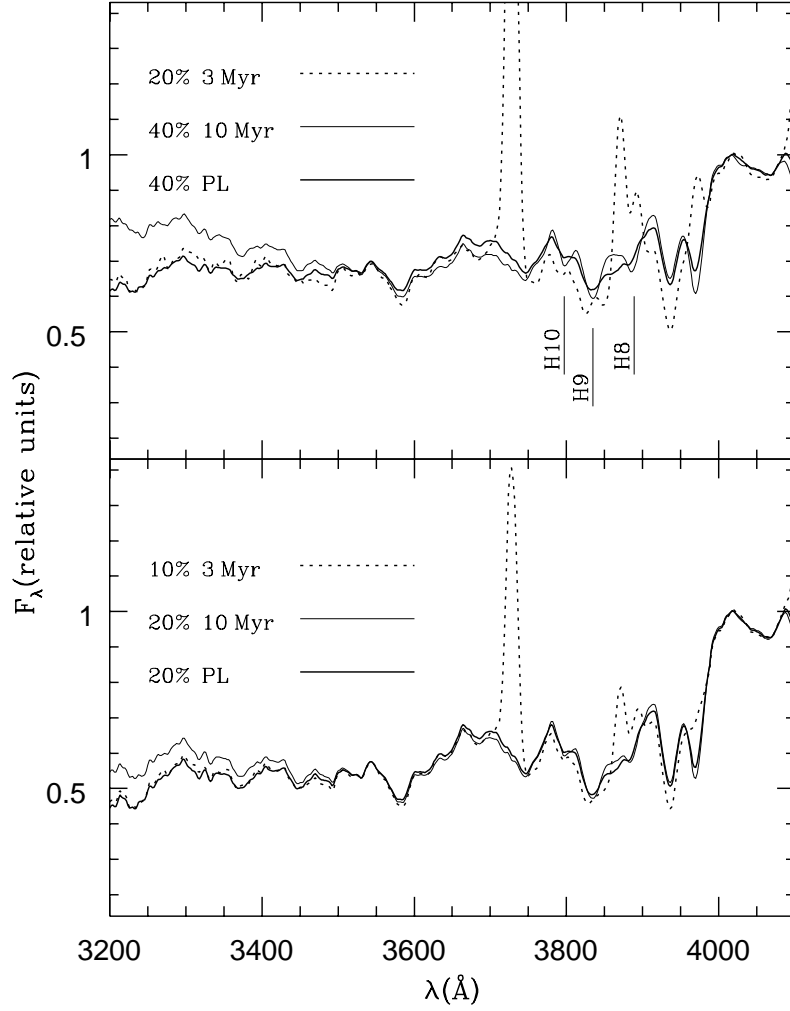


Fig. 18.— Comparison between model spectra constructed combining the bulge template with: (i) a PL (heavy line) contributing with 20% (bottom panel) and 40% (upper panel) of the flux at $\lambda 4020\text{\AA}$; (ii) a 10 Myr population template (thin line) with the same contribution as the PL; and (iii) a 3 Myr population template (dotted line) contributing with 10% (bottom panel) and 20% (upper panel) of the flux at $\lambda 4020\text{\AA}$.

Age	M/L _V	L _{λ4020}
3 Myr	0.030	1134.0
10 Myr	0.007	3354.1
50 Myr	0.054	504.4
100 Myr	0.260	97.1
500 Myr	0.310	63.9
1 Gyr	2.19	6.8
10 Gyr	8.6	1.0

Table 1: Template ages, mass-to-light ratios in V and relative luminosity at $\lambda 4020\text{\AA}$

Name	$\lambda 3660/4020$	W_C	W_{H9}	W_{CaIIK}	Scale
		(Å)	(Å)	(Å)	(pc/arcsec)
NGC1358	0.51	4.5	18.5	18.6	257
MGC1386	0.52	2.5	12.9	14.0	48
NGC3081	0.69	3.5	12.8	14.0	140
NGC5135	0.74	0.4	4.0	2.7	256
NGC5643	0.55	0.8	7.4	9.5	69
NGC6300	0.54	3.0	12.9	15.8	63
NGC6890	0.72	3.0	10.1	13.7	159
NGC7130	0.93	0.5	3.1	3.3	314
NGC7582	0.62	0.7	4.1	3.7	100
Mrk348	0.72	2.4	8.6	13.0	302
Mrk573	0.70	3.7	11.8	15.1	334
Mrk607	0.63	2.9	12.8	14.3	176
Mrk1210	0.83	1.6	em	9.5	253
CGCG420-015	0.57	2.6	9.8	13.8	570
IC1816	0.66	2.2	6.9	12.8	328
IRAS11215-2806	0.55	1.4	7.4	11.8	262
MCG-05-27-013	0.67	2.9	11.6	15.1	470
Fairall316	0.57	4.6	17.9	18.2	308
ESO417-G6	0.59	3.5	13.3	15.2	310
ESO362-G8	0.52	0.1	7.4	5.8	298
3C33	0.60	2.4	12.9	15.2	1114
P0349-27	0.60	4.4	16.1	18.5	1240
P0634-20	0.66	3.4	16.2	17.9	1055

Table 2: Near-UV measurements and scale of the Sample

Galaxy	RC3	Malkan et al.
Mrk 607	Sa	Sb
NGC 1386	SB0	Sbc
CGCG 420-015	?	Sa
ESO 362-G8	S0	Sa
Mrk 1210	S?	Sa
IRAS 11215-2806	?	S0
MCG-05-27-013	SBa	Sb
NGC 5135	SBab	Sc
NGC 6300	SBb	Sd
NGC 7130	Sa	Sd

Table 3: Previous and new classifications